Journal of New Technology and Materials (JNTM)

J. New Technol. Mater.

Vol. 11, N°02 (2021)42-47

OEB Univ. Publish. Co.

Synthesis of SnO_2 thin layers by sol-gel programmed dip coating method: Effect of deposition precursor on structural and optical properties

Y. Mouchaal[a,b*], S. Benkoula[a] and A. Khelil[a]

[a]*Laboratory of Thin Films Physics and Materials for Electronics (LPCMME), Faculty of Exact and Applied Sciences, Oran University 1 Ahmed Benbella, BP 1524 Oran El-Mnaouer, Algeria*

[b]*Département of Physics, Faculty of exact sciences, University Mustapha Stambouli of Mascara, B.P. 305, Mascara 29000, Algeria.*

*Corresponding author, email: younes.mouchaal@univ-mascara.dz

Selected paper of JMSM-2020, received date: Aug. 01, 2021 ; accepted date: Sep. 30, 2021

Abstract

Tin dioxide (SnO_2) is a material belonging to the family of transparent and conductive oxides (OTC). It has the advantage of being non-toxic and abundant on Earth, having good optical transmission and high electrical conductivity as a transparent conductive layer. Important advances have been made in its application in the field of solar cells. This paper presents details on study of dip coated tin oxide SnO_2 thin layers prepared on glass substrates. It has been shown that he heat treatment effect on opto-electrical structural and morphological. X-rays diffraction analysis revealed that a formation of tetragonal cassiterite structure with a preferred growth orientation according to (101) plane with significant effect of deposition precursor concentration on crystallites size. The SEM images showed that the films morphology depends on precursor concentration and is controlled by annealing at 400°C, where, it becomes smoother for higher concentration starting from 0.2 mol. UV-Visible spectroscopy has shown the high transparency of SnO_2 films ranging in the domains (65%–75%). For all films, the optical band gap energy varies randomly with the precursor concentration and has been estimated; conversely, it increases from 3.73 eV to 3.77 eV.

Keywords: SnO_2, Dip Coating, XRD, SEM, cassiterite structure.

1. Introduction

Stannic oxide or tin dioxide SnO_2 is a substance belonging to the ceramics family of transparent semiconductors. Tin oxide is a transparent conductive oxide known as (TCO), it is non-toxic and plentiful. It has the shape of a mineral cassiterite, with a tetragonal crystal lattice similar to the structure of a rutile [1, 2]. It is a broad band gap (3.6-3.8 eV) n-type semiconductor [3] and has strong electrical conductivity, with outstanding thermal and optical properties [4]. Tin oxide is also known for its chemical stability providing it imparts capability of lifetime improvement of structures [5]. Caracteristics structure make tin oxide a suitable candidate for various applications in transparent electrodes/window layers in solar cells, gas sensors, diodes and anodes in lithium batteries [6].

Many tin oxide deposition techniques are possible, such as sputtering, thermal evaporation, spin coating and dip coating [7-11]. Dip coating has the following advantages among these methods: it is a simple and inexpensive method of deposition, able to achieve a smooth, transparent and homogeneous thickness [12].

However, in order to be able to use it for various applications, regulation of its physical properties remains very important, such as gas sensors[13, 14], oxidation catalysts[15, 16], transparent conducting electrodes for flat-panel displays[17, 18] and photovoltaic cells[19].

In developing assisted transparent metal oxide films, the challenges are the synthesis of an ideally transparent, stable and homogenous SnO_2 structures. The optimized morphology, as well as its conformal coating, is simple and scalable with a very thin layer. In order to prepare a dimensionally stable tin oxide thin film with a very low energy consumption process, we present a scalable approach.

On the deposition and properties of SnO_2 thin films, this paper states. The structural and morphological experiments were associated with the optical features. The purpose of this study is to demonstrate the effect of the concentration of deposition precursors on the performance of tin oxide thin films using the programmed dip coating deposition method.

2. Material and methods

2.1. Dip-coating deposition (DCD) parameters

Tin dioxide thin films are prepared by DCD root using microscopic glass (Heinz Herenz, of 2 cm × 2 cm) as substrate. The cleaning process consists on successive immersion in an ultrasonic bath in acetone and ethanol

then drying in air. This cleaning process removes stains of grease and impurities stuck to the surface of the substrate confirmed by observation with optical microscopy.

There are several methods of preparing a precursor for the deposition of thin layers of SnO_2, in this work, our thin layers have been prepared from a precursor solution containing the following reagents:

• Tin chloride ($SnCl_4 \cdot 2H_2O$, 99.99%, Sigma Aldrich) fine gray powder, its molecular mass is M = 189 (g / mole).

• Methanol (CH_3OH, 99.99%, Sigma Aldrich).

In order to prevent the formation of hydroxide precipitates, a quantity of 0.02 mL of acetic acid (99.99 percent, Sigma Aldrich) was applied to the precursor solutions for SnO_2 deposition. The precursor mixture was subsequently stirred using a magnetic stirrer at low speed at a temperature of 60 ° C for 20 minutes in order to ensure good dissolution of all the elements and to avoid possible precipitation of compounds, which is detrimental to the morphology of the thin layers to be deposited.

For our investigation consisting in study of precursor concentration effect on the physicochemical properties of thin layers of transparent oxide conductor SnO_2, we made deposits from several solutions of different concentrations then annealed at 400°C. We summarize in Table 1 the deposition parameters of studied films.

Table1: Conditions for the Dip Coating deposited tin oxide films.

Dip coating parameters	Experimental value
Immersion speed	2 mm / s
Withdrawal speed	1 mm / s
Immersion time	10 s
Pre-annealing time	15 min
Pre-annealing Temperature	190 ° C
Number of cycles	5 times
Annealing Temperature	500 ° C
annealing time	5h

2.2. Films characterization

A UV-vis spectro-photometer (Perkin-Elmer Lambda 950 UV-Vis-NIR) with an integrated sphere with a scan rate of 60 nm/min was used to perform optical measurements at room temperature (lamp changes at 326 nm). The visible spectral range of the optical transmission measurements was estimated within 350-1100 visible included range.

A field emission scanning electron microscope (SEM, JEOL F-7600) was used to observe the surface topography of the structures. With its wide angle backscattered detector (LABE), only the powerful resolution of this field emission SEM enabled us to obtain images at such a high magnification in backscattered mode.

An energy dispersive X-ray spectrometer (Ultra Dry, Noran System 7, NSS Model ,20,00,000 counts/s) combined to the used SEM conducted the elemental analysis of the films.

X-ray diffraction (XRD, Bruker D8 Discover Advanced Diffrac-tometer) using Cu K_α radiation (λ= 0.15405 nm) allowed structure examination of the deposited thin films and the scan-step size is 0.015.

3. Results

3.1 Structural properties

Table 2: Variation of the crystallite size of SnO2 dip coated thin films as function of precursor concentration at annealing 400°C for (310) preferential orientation.

Deposition parameters C (M) Annealing T	(2θ) (deg)	crystallite size (nm)
0.05M 400 °C	64.72	18
0.10 M 400 °C	64.71	19.3
0.15 M 400 °C	64.73	20.5
0.20 M 400 °C	64.7o	24.5
0.25 M 400 °C	64.7o	22.3
0.2 M Not annealed	64.72	14.9

Figure 2 shows the XRD patterns of the SnO_2 thin films deposited by dip coating and annealing at 400 °C for 60 min with various deposition concentrations. The polycrystalline nature of the SnO_2 films with a tetragonal crystal structure is revealed by X-ray diffraction spectra.
From XRD results we noticed that the deposited films annealed at 400°C for 60 min crystalizes from a deposition concentration of 0.1 M which is explained by the fact that from this concentration there will be a continuity of deposit on the surface of the substrates and the limited effects become negligible [20-22] .

The curve shows four diffraction peaks corresponding to (110), (101), (200) and (200), respectively, for the SnO_2 dip-coated films. The increase in precursor deposition concentration contributes to the emergence of other peaks observed at 33.8o, 51.7o, 57.8o, 64.7o, 78.7o, corresponding to planes (101), (211), (002), (310), (202) respectively. This shows the formation of the SnO_2 cassiterite tetragonal structure as per JCPDS (No 00-041-1445)[23, 24].

The crystallite size of SnO_2 films determined by Scherrer (Relatin1) is shown in Table 2. As the precursor concentration increased, the size of crystallite increased and the full width at half limit (FWHM) of the diffraction peaks decreased, as shown in Figure 2. This conduct is due to growing crystalline growth and reducing the boundary of grains with increasing the precursor concentration. These findings are consistent with earlier results [25,26].

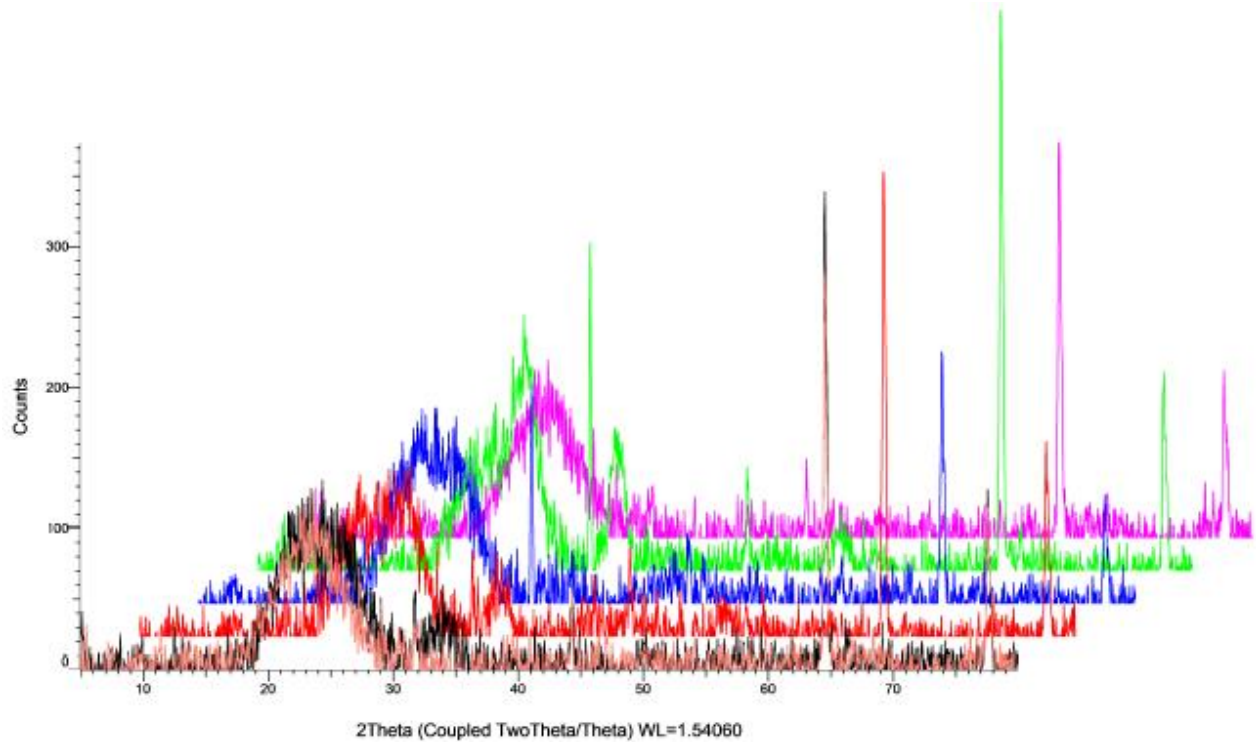

Figure 1. Optical transmittance of dip coated SnO_2 thin films for different deposition precursor concentration.

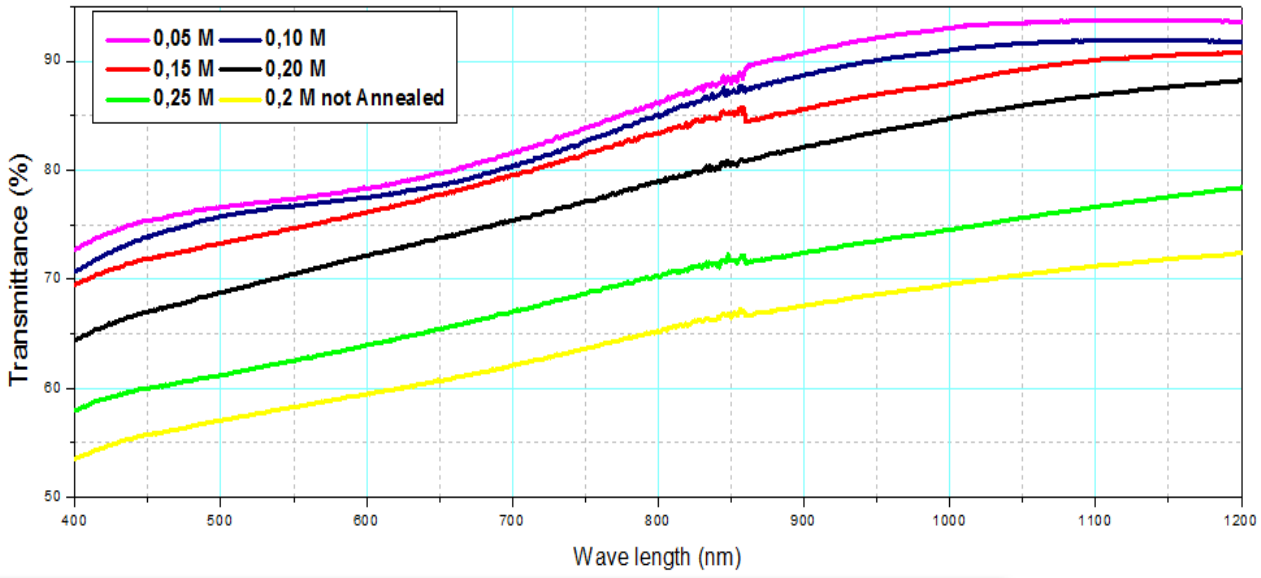

Figure 2. Optical transmission of dip coated SnO_2 thin films for different deposition precursor

The Scherer equation was used to measure the crystallite size [27, 28].

$$D = k\lambda/\beta cos\beta\theta \quad (1)$$

Where k is a fixed value that should be taken as 0.9, λ the X-ray wavelength 1.5406Å, β the full width at half maximum FWHM and and θ Bragg diffraction angle of the XRD peak.

3.2 Morphological properties

3.3. Optical properties

Since the optical properties of transparent electrodes are important in the reliability of the devices, the control of the optical characteristics is essential for the study of thin films of metal oxides. For this, we gradually characterized our thin layers by a UV-Visible spectrophotometer. We are interested in optical transmission measurements in the visible-near UV domains and the variation of the absorption coefficient as a function of light energy. The optical transmission spectrum of dip coated SnO_2 thin films for different precursor concentration is shown in Figure 2.

The transmission spectrum average varies between 55 and 95% depending on the wavelength between 400 and 1200 nm for samples prepared at different concentration.

The 0.2 and 0.25 M samples showed the most adequate transmission around 75% in the visible range (400-800 nm) then by increasing the concentration, the optical transmission decreases, on the other hand it is significantly improved following annealing at temperature of 400 ° C. The drop in transmission makes sense, as with increasing concentration there is more SnO_2 material in the films. Improved transmission through annealing is achieved through restructuring and standardization of deposited thin layers; this confirms the role of thermal annealing in improving the optical properties following the crystalline organization of the Sn-O tissue confirmed by previous crystallographic analysis.

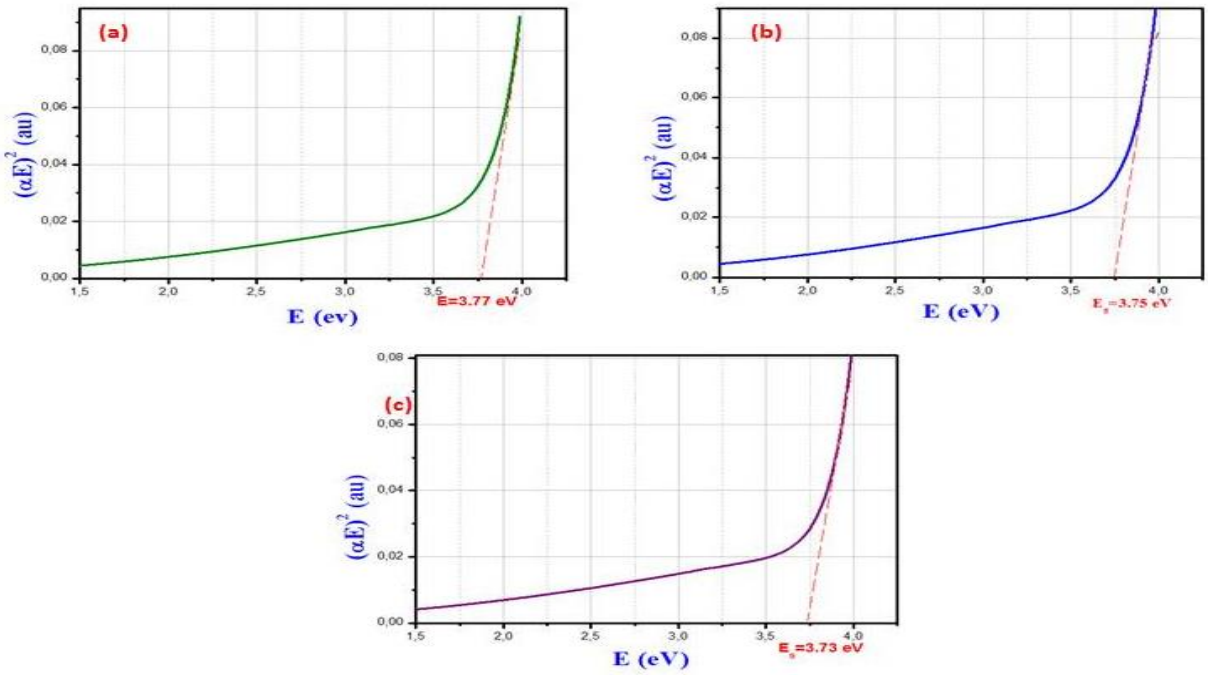

Figure 3. Curves $(\alpha E)^2$ entity variation as a function of the photons energies for deferent concentrations of SnO_2 deposition precursors, and deduction of their electron band gap.

The energy gap of the SnO_2 band is defined by the graph $(\alpha h\nu)^2$ as a function of the photon energy hν, the absorption coefficient and the optical gap can be determined by the certified direct transition relation[27]:

$$\alpha = (\ln(1-R)^2/T))/d \qquad (2)$$

$$(\alpha h\nu)^2 = A\,(h\nu - Eg)^2 \qquad (3)$$

Extrapolating the curve for $(\alpha\hbar\omega)^2=0$, which corresponds to the decreasing linear component, to the x-axis, we get the energy of the band gap (E_g).

The curves shown in Figure 3 represent the square of the absorption coefficient as a function of the photon energy for three deferent concentrations for samples 0.1, 0.2 and 0.25 annealed at 400 ° C. extrapolation of the linear part of curves (a), (b) and (c) gives E_g values equal to 3.77ev, 7.75ev and 3.73 eV respectively, these values of the gap are in good agreement with those of literature [28]. We notice that the optical gap decreases with the concentration of the precursor SnO_2, until it tends towards the value of Eg specific to SnO_2 when we obtain completely compact and continuous films.

The surface of the SnO_2 samples seen by SEM scanning electron microscope shown in figure 4 shows that it is relatively smooth, where we observe the presence of grain of different color on the surface with an increase in their sizes depending on the concentration of precursor of

deposit. These observations show that the thin layers are formed of small crystallites distributed randomly on the surface and in volume which increases their size as a function of the concentration of deposition precursor.

From the SEM observations we also note that the SnO_2 films have a granular form distributed in surface and in volume. By increasing the concentration of the deposition precursor we notice an approximation and slight increase in their size, this is due to the fact that when we increase the concentration we increase the compactness of the SnO_2 tissue and we tend towards continuous SnO_2 configurations free of voids (empty area on the film).

The average RMS roughness calculated is of the order of 12.1, 19.6, 23.8 and 33.0 nm respectively for the 4 concentrations studied, we can conclude that the third concentration (0.2 mol / l) is optimal among that tested, given that the roughness of these films meet the specifications for transparent anodes.

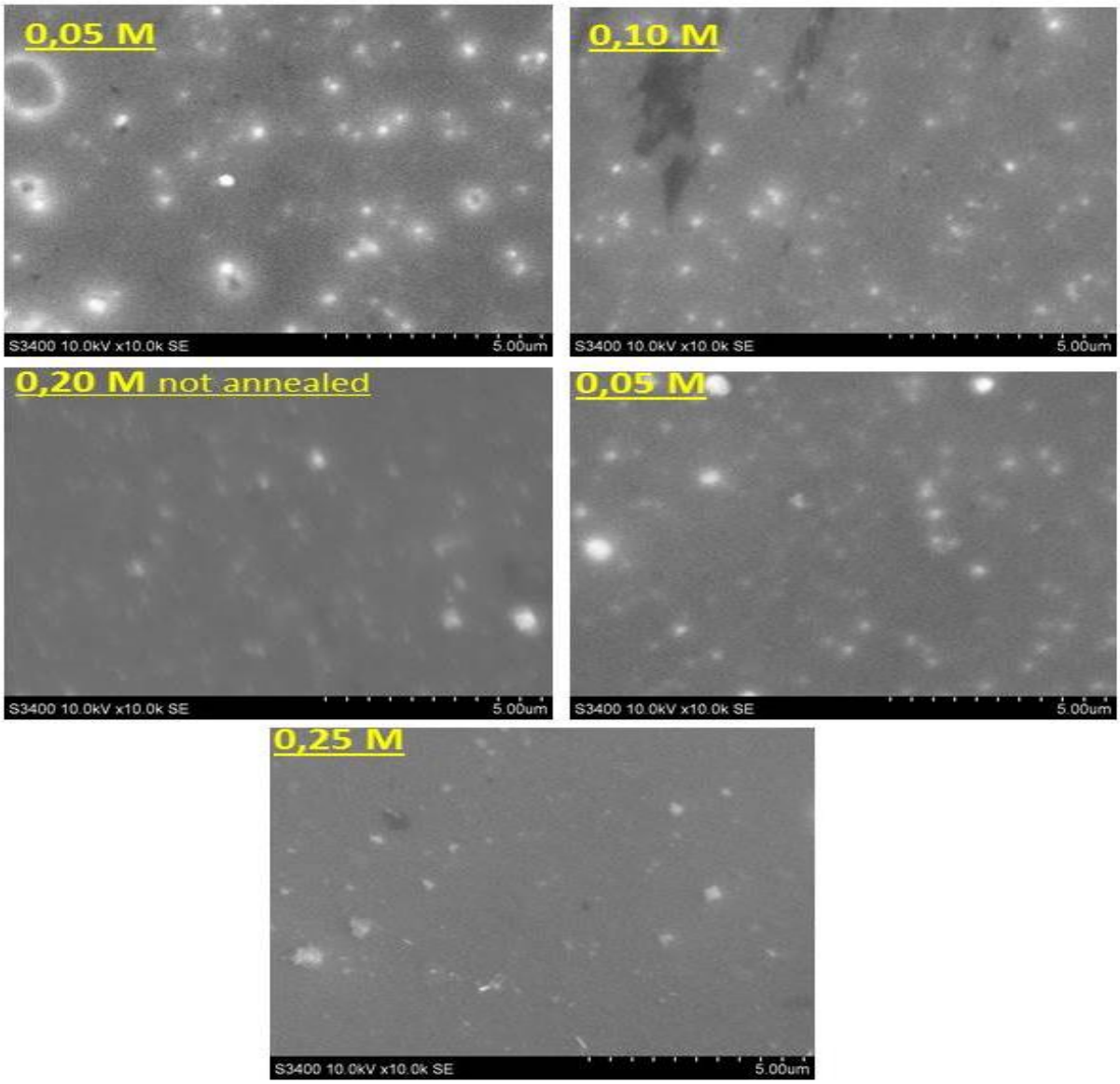

Figure 4. SEM surface images of Sno_2thin films from deferent concentrations of deposition precursors,

4. Conclusion

In this work, using a dip coating technique, we concentrated on the deposition of SnO_2 thin films. We studied the impact of thermal annealing and precursor concentration on structural, morphological and optical properties.

The optical optimization of the deposit precursor concentration of SnO_2 thin layers allows obtaining of highly transparent films with an average transmission varying between 66 and 76%, the electronic gap deduced from the optical measurements is around 3.7 eV, being in good agreement with the bibliography.

The deposited films showed the formation of the SnO_2 cassiterite tetragonal structure. The increase in precursor deposition concentration contributes to the emergence of other XRD peaks and an improvement of the surface grains until a homogeneous and compact surface is obtained from a concentration of deposit precursor of 0.2 M.

In conclusion of this work, we have optimized and obtained homogeneous films with modular physical properties based on an abundant and non-toxic material, SnO_2, with characteristics comparable to those of other metal oxides obtained with expensive techniques, which opens the way for such materials to be concurrent to be integrated as a buffer layer or anode in optoelectronic devices, in particular organic solar cells.

Many perspectives were inspired by completing this work. Primarily the manufacture of flexible solar cells based on fabricated anodes and the use of our cost-effective films for the protection, stabilization and optimization of transparent electrodes and optoelectronic devices.

Acknowledgments

The authors thank the JMSMS'2020 organizing and scientific committee for their assistance and efforts.

The authors acknowledge funding from the European Community ERANETMED_ENERG-11-196: Project NInFFE.

Dr Y. MOUCHAAL would like to thank Pr A Duta and Pr D Perniu for their assistance, XRD and SEM analysis.

References

[1] B. Cheng, J M. Russell, W. Shi, L. Zhang, ET. Samulski, JACS 126 (2004) 5972–3
[2] L.A. Patil, M.D. Shinde, A.R. Bari, V.V. Deo, Sensors and Actuators B 143 (2009) 270–277.
[3] L. Qiang, S. Jiudi Sun, S. Yudan, R. Zonghuan, L. Chao, L. Jingwei. L. Famei Wanga L. Wei, S. Tao, K. Paul Chu, Optical Materials 102 (2020) 109800.
[4] J. Zhao, L.H. Huo, S. Gao, J.G. Zhao Hand, Sensors Actuators B: Chemical 115 (2006) 460–4.
[5] D. Haouanoh, R. Zaïr TalaIghil, M. Toubane, F. Bensouici, K. Mokeddem, Mater. Res. Express 6 (2019) 086422
[6] Y. Wang, Z. Chen, D. Xu, Z. Yi, X. Chen, J. Chen, Y. Tang, P. Wu, G. Li, Y. Yi, Results Phys. 16 (2020) 102951.
[7] J. Montero, J. Herrero, C. Guillén, Sol. Energy Mater. Sol. Cells 94 (2010) 612–6.
[8] Sun S, Meng G, Zhang G, Gao T, Geng B, Zhang L and Zuo J, Chem. Phys. Lett. 376 (2003) 103–7
[9] M. Ocana, C. Serna, Spectrochimica Acta Part A: Molecular Spectroscopy 47 (1991) 765–74.
[10] D. Yoo, J. Tamaki, S. Park, N. Miura,N. Yamazoe, J. Mater. Sci. Lett 14 (1995) 1391–3.
[11] J. Zhao, L.H. Huo, S. Gao, H. Zhao, Z. Hand, J.G Zhao, Sensors Actuators B: Chemical 115 (2006) 460–4
[12] M. Toubane, R. Tala-Ighil, F. Bensouici, M. Bououdina, W. Cai, S. Liu, M. Souier, A. Iratni, Ceram. Int 42 (2016) 9673–85.
[13] M. Moalaghi Mohsen G. Alireza Ranjkesh Faramarz, H. Babaei, Materials Letters 263 (2020) 127196.
[14] M. A. Basyooni, Y. R. Eker, M. Yilmaz, Superlattices and Microstructures 140 (2020) 106465.
[15] A. Hartig-Weiss, M. Miller, H. Beyer, A. Schmitt, A. Siebel, A. T. S. Freiberg, H. A. Gasteiger, H. A. El-Sayed, ACS Appl. Nano *Mater* 3 (2020) 2185–2196
[16] M.M. Bagheri-Mohagheghi, M. Shokooh-Saremi, Physica B 405 (2010)4205–4210.
[17] J.P. Chatelon, C. Terrier, E. Bernstein, R. Berjoan, J.A. Roger, Thin Solid Films 247(1994) 162–168.
[18] L.P. Ravaro, D.I. dos Santos, L.V.A. Scalvi, J. Phys. Chem. Solids 70 (2009)1312–1316.
[19] C.E. Benouis, M. Benhalilibaa, F. Yakuphanoglu, A. Tiburcio Silver, M.S. Aida, A.Sanchez Juarez, Synth. Met. 161 (2011) 1509–1516.
[20] R. Mariappan, V. Ponnuswamy, P. Suresh, N. Ashok, P. Jayamurugan, A. Chandra Bose, Superlattices and Microstructures 71 (2014) 238–249.
[21] Y. Mouchaal, A. Khelil Eur. Phys. J. Appl. Phys 87 (2019) 31302.
[22] A.A. Rifat, R. Ahmed, G.A. Mahdiraji, A. Mahamd, F.R.M. Adikan, Highly IEEE Sensor 17 (9) (2017) 2776–2783
[23] A.Z. Al-Janaby, H.S. Al-Jumaili, IJRET 3 (2016) 40–5
[24] F. Huang, F. Pu, X. Lu, H. Zhang, Y. Xia,Z. HuangWand, Sensors Actuators B: Chemical 183 (2013) 601–7
[25] A. Gadkari, T.J. Shinde, P.N. Vasambekar, P.N, Sensors and Actuators B , 178 (2013) 34-39.
[26] Y. Mouchaal A. Enesca, C Mihoreanu, A. Khelil, A. Duta, Materials Science and Engineering: B, 199 (2015) 22-29.
[27] S. M.H. Al-Jawad, Materials Science in Semiconductor Processing 67 (2017) 75–83.
[28] S.M.H. AL-Jawad, A.A. Taha, M. M. Salim Optik 142 (2017) 42–53.